MOUNTING FOAMS: MAKING OF SPECIMENS AND MECHANICAL TESTING

ZBYNEK PASKA[1], JAROSLAV ROJICEK[1], MARTIN FUSEK[1], FRANTISEK FOJTIK[1], DAGMAR LICKOVA[1], JAKUB CIENCIALA[1]

[1]Department of Applied Mechanics, Faculty of Mechanical Engineering, Ostrava-Poruba, Czech Republic

[2]Department of Robotics, Faculty of Mechanical Engineering, Ostrava-Poruba, Czech Republic

DOI: 10.17973/MMSJ.2022_10_2022118

zbynek.paska@vsb.cz

The article deals with the design of the technology of production of polyurethane foam (PU) specimens and with their mechanical testing. A simple procedure is proposed to produce specimens with complex shapes. The procedure is tested on two different mounting foams. These specimens were subjected to several experiments. The article presents experimental results for only one mounting foam. The tests were performed on a Testometric M500-50CT testing machine. Specifically, these are a tensile/compression test, a 3-point bending test, a shear test, and a modified indentation test. For each specimen, the displacement was also measured in the selected area with Digital Image Correlation Method. These measured data are presented in the article.

KEYWORDS

Mounting foam, make a specimen, experiments, tension/compression, bending, shear, modified indentation

1 INTRODUCTION

The work is thematically related to the article [Paska 2020], which deals with the design of the robot manipulator arm using topological optimization for 3D printing. The connection of these arms is often realised by HELICOIL® inserts. A simple analysis of this type of connection can be found in the article [Paska 2021].

A manipulator arm composed of a set of sheet metal components and optimized by a genetic algorithm was presented in [Rojicek 2021]. The resulting structure was a frame, that meets a given set of constraints. Some structures may have a buckling problem that impairs the properties of these structures. This problem occurs, for example, in frame, truss or thin-walled structures [Rojicek 2021]. One way to overcome these problems is to fill these structures with foam, which is lightweight, freely available, and easy to use. It is expected that foam filling will also have a positive effect on damping potential vibrations. In different areas of research or teaching, often only one manipulator, or only a part of it, is designed. The aim is to make a design by the chosen method (shape or topology optimization), to achieve certain properties (e.g., stiffness), or to subject the resulting design to experimental analysis. The use of mounting foams, which are also available at a low cost, can be a simple option. The problem is that the mechanical properties of mounting foams are not generally known.

The foams are characterized by specific properties. A very important property of foams is their ability to absorb deformation energy. There are a lot of foams that have an interesting uses or practical applications [Kumar 1993]. They are therefore used as part of sandwich components in the aerospace and railroad industries [Zenkert 2009]. In the automotive industry, foams are used as a filler material for car bumpers [Morton 2020]. Another key property of foams is their density [Bhagavathula 2022]. The properties of foams, such as the relative number of open cells in the volume, cell size, cell shape, and cell wall thickness [Srivastava 2014], have an effect to their behaviour. Most of these parameters are related to the type of foam and can be significantly influenced by the manufacturing technology.

A basic classification of foams can be made based on materials such as metal foams [Dukhan 2013], polymer foams [Eaves 2004], [Gama 2004], or ceramic foams [Bhaduri 1994]. A subdivision in terms of their application can be used [Anirudh 2022], [Singh 2018] or structure such as open cells [Yang 2015] or closed cells [Huo 2016]. The structure of foams is very complicated, but in some cases, it can be modelled. For example, the modelling of foam structures is presented in [Jiang 2020], for structures generated by 3D printing [Marx 2017], and for metal foams in [Wu 2010]. In this case, the material (model and its parameters) and the structure can be solved separately. Another approach is based on constitutive equations for metals modified for foams. A more detailed breakdown, including literature references, can be found, for example, in [Srivastava 2014]. This paper does not deal with Finite Element Analyse of foams and therefore we will not discuss in detail the material models, their analyses, simulations, or applications.

We did not find any literature on the fabrication of test specimens from mounting foams. On the other hand, in literature can be found articles dealing with foams experiments. Experiments have been performed based on classical tensile loading, including cyclic tensile loading [Yousaf 2022] (standard ISO 37:2017) or dynamic fracture tests [Kabir 2006] (standard ASTM D5045). Compression tests are introduced in [Li 2021] (standard ASTM D1621-16). Indentation or impact tests are also used for foams, see [Gilchrist 2001]. More complex experiments for multiaxial tests can be found in [Donnard 2018] (standard NF EN ISO 1798). The behaviour of foams often falls in the viscoelastic range [Henriques 2020] (standard ISO 6721-7 (2019)), and the complex behaviour of foams at failure or at different temperatures is addressed in [Lee 2020].

Validation is an important part of simulations, and necessary step for practical application of material models. [Rojicek 2021/3] was presented using data from DIC (Digital Image Correlation method) measurement to validation of behaviour of material models and its parameters.

The main objective of the paper is the production of mounting foam specimens, the design, and realisation of mechanical tests to obtain material data. In the paper, the results are presented for only one brand of mounting foam.

2 MOUNTING FOAMS

There are a few foams available on the market that differ in composition, behaviour and use. Only one type of foam is used in this article, but we assume that presented approach can be used for foams with similar properties.

The tubular PU mounting foam "Den Braven" (PUMFD) with a reduced expansion is used to make the specimens [Den Braven 2022]. The foam is used for insulation, waterproofing, cavity, and joint filling. It is a one-component semi-rigid polyurethane (PU) foam. The manufacturer's website provides more detailed information on the parameters of the foam. According to the manufacturer, the density of the foam is 20 to 30 kg m^{-3}. The density is very important for the mechanical behaviour of the foam. The cell structure of the foam is closed. The colour of the foam is green (see Fig. 1a). The mechanical properties are not specified by the manufacturer.

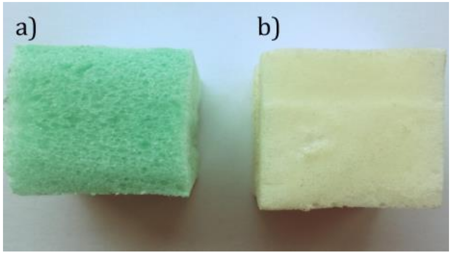

Figure 1. Two types of foams tested for specimen production

Furthermore, the mounting foam "SOUDAL" [SOUDAL 2011] was tested for specimen production. It is low expansion mounting foam. The colour of this mounting foam is white (see Fig. 1b). The cell structure of this foam is also closed-cell. Usable specimens were also produced from this mounting foam. In this paper, only the results for foam "Den Braven" are presented below.

3 DESIGN OF EXPERIMENTS

The experimental design is based on the literature presented in the Introduction. The Testometric M500-50CT testing machine [Testometric 2021] was chosen to perform the tests. In addition, a DIC optical measurement system was used to obtain the second data set.

The following tests were performed:

- Tensile test (ISO 1798), the rate 4 mm min^{-1}. The tensile specimen was loaded to failure.
- Compression test (ASTM D3574-03), the rate 4 mm min^{-1}, and 40 mm min^{-1}. A cube shaped specimen with a side length of 30 mm was placed into the machine between two parallel plates. The specimen is compressed by 25 mm and then released.
- 3-point bending test, the rate 4 mm min^{-1} (ASTM D5379-93). A specified test fixture was used. There is a distance of 150 mm between the lower supports, in the middle between them is the loading member.
- Shear test ASTM D5379-93, the rate 4 mm min^{-1}. Simply test fixture was designed for the experiment, see Fig. 2 The fixture was manufactured by 3D printing from PETG (PRUSA POLYMERS by JOSEF PRUSA) [Prusa 2022].
- Indentation test [Gilchrist 2001] ISO 14577-1, the rate 4 mm min^{-1}. Unlike the classical test, the fixture for 3 point bending test was used for indentation (a cylinder 25 mm in diameter). The foam specimen was placed on a flat plate and a cylinder (indenter) was pressed on the top side of the specimen. This type of indenter produced a more distinct strain pattern for the DIC measurement than, for example, a sphere indenter.

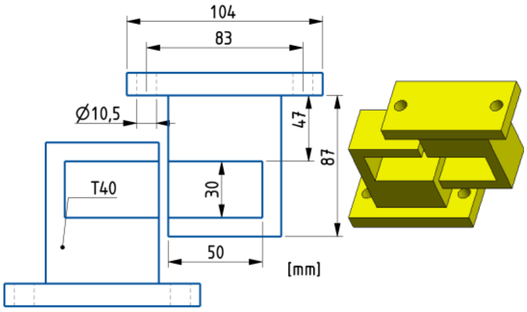

Figure 2. Shear test fixture, the test is based on the standard ASTM D5379-93 for notched specimens.

All tests were carried out at normal room temperature. The loading conditions can be divided into two groups:

1) loading to failure (tensile test, shear test),
2) loading with unloading (compression test, bending test and indentation test).

The DIC method requires covering the specimen surface with a contrast pattern. The contrast patern was applied to all measured specimens, and is presented in the next chapters.

4 SPECIMENS PRODUCTION

Two approaches of specimen fabrication were tested: **The first approach** was to create specimens with a circular cross-section. For their production we designed closed moulds (for 3D printing). However, this approach was not successful, because most conventional PU foams require access to air and moisture. Creating a non-adhesive interlayer between the foam and the mould to ensure convenient removal of the specimen from the mould was also problematic. As the foam expanded, a separating powder was often wiped off and the specimen and mould stuck together. This approach was only successful in producing specimens for compression tests, which are not presented here. Note: Closed moulds may not be problematic when using two-component mounting foams that harden by chemical reaction and do not require access to air and moisture. But even in this case, the biggest problem is the formation of the non-adhesive layer.

The second approach was to make specimens with square or rectangular cross-sections, again using 3D-printed moulds. Two opposite sides of the mould were coated with a release powder layer. The other two sides were mechanically separated from the mould by cutting (deburring knife, saw blade, etc.). The mould was designed to guide the cutting tool to ensure dimensional accuracy of the specimens. However, this process produces more waste material.

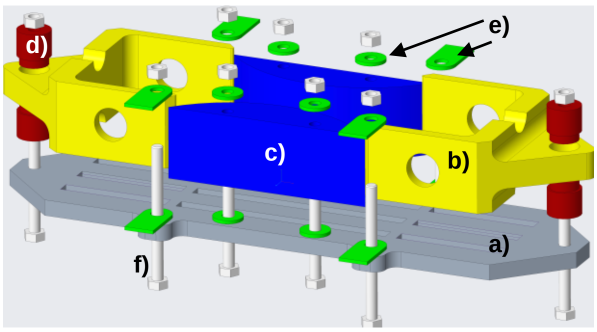

Figure 3. Mould to produce tensile specimens (plate shown only once)

The manufacturing process for the tensile specimens is described as an example. The mould must generally meet several basic parameters:

- It must have enough openings for the expansion of the excess foam and for the access of air and moisture.
- The mould must have the correct geometry of the specimen and allow mechanical cutting of the specimen.
- The mould should be reusable.
- The mould may contain parts designed to attach the specimen to the testing machine (for tensile testing).

The mould tensile specimen is shown in Fig. 3. It consists of the following parts:

a) Two support plates. The plates determine the position of all other parts and allow the excess foam to escape thanks to the openings.
b) Two clamping parts are used to connect the foam to the testing machine. They must be designed in such a way that the strength of their connection to the foam is sufficient to avoid separating them during the experiment. The used foam holds itself in the clamping parts by its own adhesion.
c) Two semi-circular parts. These parts determine the shape of the test area of the specimen and a separation powder has been applied to them. By changing them, you can easily create the desired shape of the test part of specimen.
d) Four pins. These pins are used to maintain proper distance between the plates and clamping part.
e) Demarcation pads that ensure the centring of the specimen and the creation of a gap for guiding the cutting tool.
f) Screws, nuts and washers for the mould assembly.

For specimen production we also need suitable separation powder and paints to create a contrast pattern for DIC measurements. When assembling the mould, it is necessary to maintain the gaps for guiding the cutting tool to remove (cut out) the specimen from the mould.

The resulting shape after application of the foam inside the mould, expansion and hardening of the foam is shown in Fig. 4. The amount of foam is difficult to estimate when applying by hand; the mould should be filled completely, and excess foam should expand freely. In the Fig. 4, the tape coated with release powder can be seen. This ensures that the semi-circular parts of the mould can be freely removed from the mounting foam.

Figure 4. Application of mounting foam into the mould

Cutting out the specimen changes its surface structure. However, this would also happen if the specimen was cut out of a foam block.

When using the shape prescribed by ISO 1798, there was an incorrect filling of the mould with foam during the production of specimens, a violation of the specimen when taken out of the mould, or when handling the specimen e.g., when inserted into the testing machine. Therefore, a more solid shape was designed. The tensile specimen with the contrast pattern (which is needed for the optical DIC measurement) is shown in Fig. 5.

Figure 5. Modification of the tensile specimen with contrast pattern

Basic dimensions of the tensile specimen are shown in Fig. 6. A shape with a slight notch in the test part of the specimen was chosen. The notch radius of the specimen is deliberately chosen to ensure that foam failure occurs in the centre of the specimen. The notch reduce the effects of stress concentration around the clamping parts.

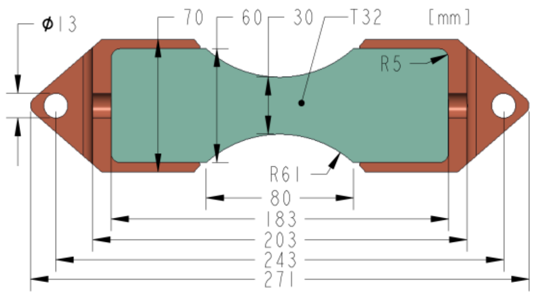

Figure 6. Dimensions of the tensile specimen

The specimens for compression, shear, 3-point bending test and indentation test were fabricated in a similar manner. Standards for a compression test, and an indentation test (ASTM D3574 – 03), 3-point bending test (ISO 178) and shear (ASTM C273, ASTM D5379-93) recommend different dimensions of test samples, which complicates their production. Therefore, the first step was to align their cross-sections to 30x30 mm. The shear test has been modified so that the same sample shape can be used. the test is based on the standard (ASTM D5379-93) for notched samples. A special preparation was designed for the shear test. The mould for this type of specimens is shown in Fig. 7. The mould consists of the following parts:

a) Two support plates,
b) two front closure elements,
c) two side closure elements,
d) washers to maintain the gap, screws, etc.

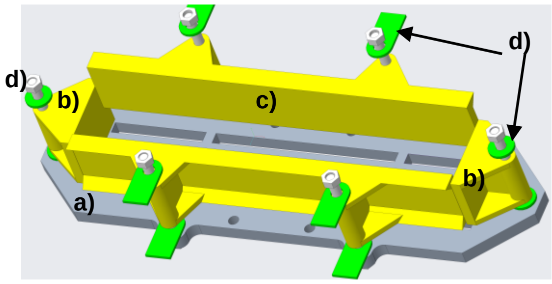

Figure 7. Mould for the production of test specimens with the dimensions 30x30x200 mm (the support plate is shown only once)

The specimen with dimensions 30x30x200 mm is also used to produce the specimens for the other tests: For the compression tests, cubes with a side length of 30 mm were used. A 30x30x100 mm block was used for the shear test and a 30x30x64 mm specimen for the indentation test.

All specimens were weighed before the tests, a Kern ABS 320-4N scales was used. The basic parameters of each specimens are listed in Tab. 1. Since only one specimen was produced for each test, no statistical evaluation was carried out. The method for determining the bulk density is regulated in EN ISO 845 (645411).

Designation	Weight [g]	Volume [mm³]	Density [kg m⁻³]
Tension spec.	6.8826	298437	23.06
Compress. spec. nu.1	0.7395	26746	27.65
Compress. spec. nu.2	0.7523	26961	27.90
Bending spec.	4.4035	180409	24.41
Shear spec.	2.4213	87775	27.59
Indent. spec.	1.5599	57522	27.12

Table 1. Parameters of specimens

It can be seen from the table that the specific densities of all specimens are within the limits specified by the manufacturer (20 to 30 kg m^{-3}). The production process can be therefore considered as correct one.

5 RESULTS OF MEASUREMENTS

The magnitude of the force as a function of time or the displacement of the crosshead of the testing machine was measured with the Testometric testing machine itself (these quantities are called primary). At the same time, the optical measurement system DIC with the software Alpha (version 2.1.52) from X-Sight s.r.o. **[Alpha SW 2022]** was used. The DIC was used to scan a section of the specimen covered by a contrast pattern. In all experiments, except for the tensile test, the DIC measurement showed the displacement of the machine crosshead as a function of time. In all experiments, the DIC measurements are used to determine all components of the strain tensor on the scanned surface as a function of time. Only in the case of the tensile test are secondary results presented here, i.e. a diagram of the dependence of the axial stress on the value of the axial relative (engineering) strain determined in the centre of the specimen by DIC measurement. The displacement values measured by DIC were used. In this case, however, it is important to link together the records of the machine and the DIC software to obtain a graphical representation of the force as a function of the displacement value.

5.1 *Tensile test*

The tensile specimen placed in the testing machine before and after the test is shown in Fig. 8.

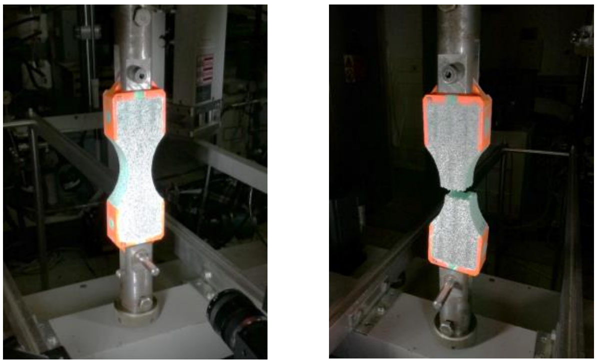

Figure 8. Tensile test: Before and after the test

Fig. 9 shows a colour map of the axial relative strain just before the specimen broke.

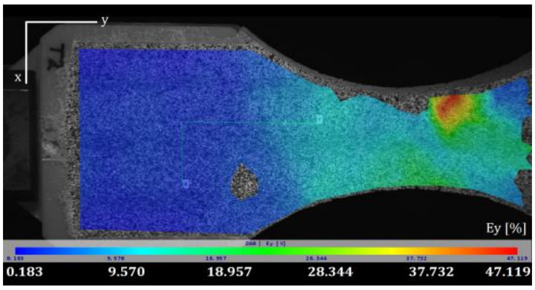

Figure 9. Map of the relative deformation Ey [%] in the y-axis direction at the bottom of the specimen

The dependence of the tensile force on the displacement value is shown in Fig. 10.

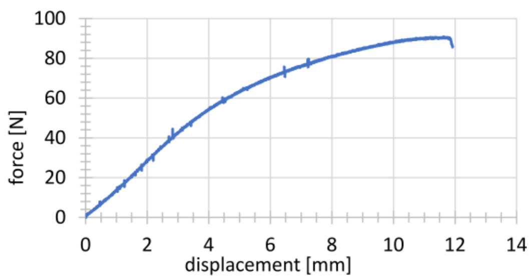

Figure 10. Dependence of the tensile force on the displacement

The resulting tensile curve is shown in Fig. 11. The stress is calculated from the smallest cross-section (30x32 mm) in the centre of the specimen. The relative strain is taken from the DIC measurement also in the centre of the specimen. The modulus of elasticity for the tensile test is 1.9 MPa.

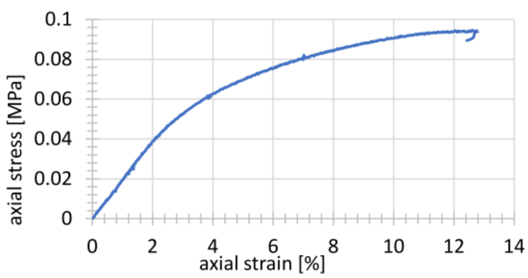

Figure 11. Graph of nominal tensile stress

5.2 *Compression test*

The compression test was performed at a speed of 4 mm min^{-1}. (Compress. spec. nu.1) and 40 mm min^{-1} (Compress. spec. nu.2). A cube-shaped specimen with a side length of 30 mm was placed in the machine between two parallel plates. The procedure for performing the compression test is shown in Fig. 12. The plates are masked so that the optical measurement is not affected by glare.

Figure 12. Compression test setup

A map of the axial deformation (in the direction of plate displacement) is shown in Fig. 13.

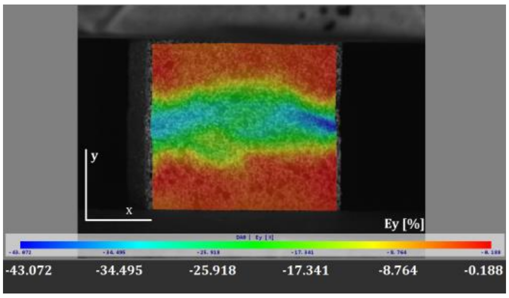

Figure 13. Axial relative deformation Ey [%] for compression test (Compress. spec. nu.2)

The dependence of the force on the displacement of the crosshead is shown in Fig. 14 for both compression speed.

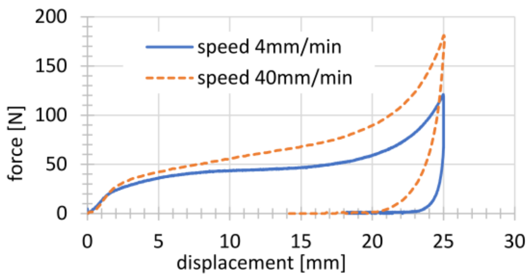

Figure 14. Compression tests for specimen nu.1 (speed 4 mm min^{-1}) and specimen nu.2 (speed 40 mm min^{-1})

5.3 *Shear test*

The graphical output of the DIC measurements for the shear test is shown in Fig. 15.

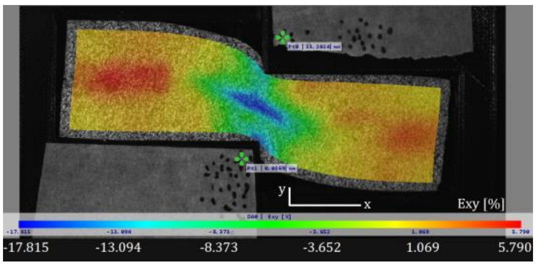

Figure 15. Shear strain map Exy [%] from DIC measurements

The shear force versus shear displacement is shown in Fig. 16.

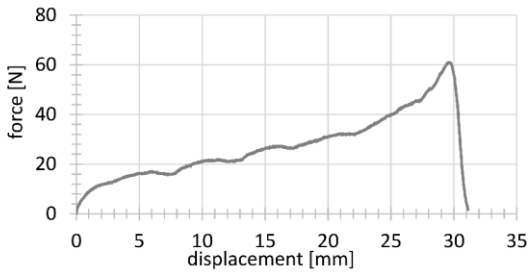

Figure 16. Dependence of shear force on crosshead displacement value

5.4 *3-point bending test*

A colour map of the relative deformation in x – axis is shown in Fig. 17.

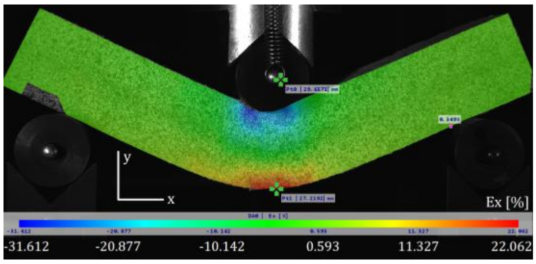

Figure 17. Map of relative deformation Ex [%]

Fig. 18 shows the magnitude of the force versus the magnitude of the deflection.

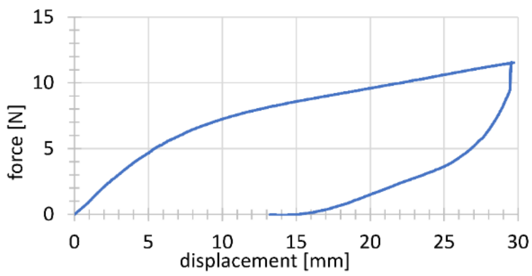

Figure 18. Graph of force dependence on crosshead displacement for bending test

5.5 Indentation test

We refer to this experiment as an indentation test, but it is rather a combination of compression and indentation testing. For illustration, a map of the relative deformation of Ey (Strain in y axis) at the time of maximum compressive force is shown in Fig. 19.

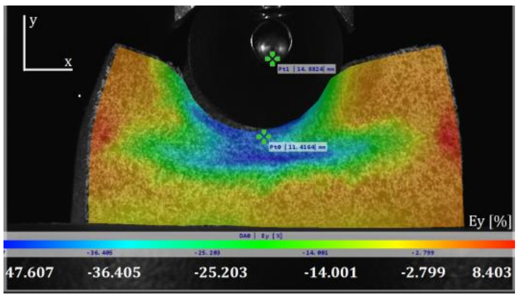

Figure 19. Map of the relative deformation Ey [%] for the indentation test

In this case, a multiaxial deformation similar to that in shear can be expected. The evaluation of the experiment in this case is more complex, but the data can be used to validate the material model or to identify its parameters using the **F**inite

Element Method Updating (FEMU) approach [Rojicek 2021/2]. The dependence of the force on the compression value of the block is shown in Fig. 20.

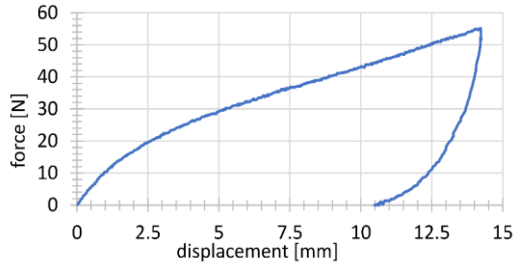

Figure 20. Dependence of force on displacement in the indentation test

6 DISCUSSION

The material behaviour of PU foams is strongly dependent on the production method and specimen processing. Air admission and humidity play an important role. The advantage of mounting foams is their easy availability and applicability. With the presented specimen production method, a larger dispersion of the measurement data is to be expected, however no statistical processing was carried out, because only one specimen was used for each tests (except of compression tests). The weight of the specimen may also be a measure of the quality of the specimen fabrication. We expect that the foams will behave similarly in practical applications on the manipulator arms. When the arm is fabricated via 3D printing [Paska 2020], a similar behaviour can be expected since the shape of the arm will be like the shape of moulds presented here. When using a frame made of sheet metal designed according to [Rojicek 2021], it will be very difficult to maintain all the necessary conditions (similar air access and humidity). The influence of the shape (number of holes) on the resulting behaviour of the foams seems to be an interesting topic for further research.

In the first stage of specimen fabrication, attempts were made to produce specimens with circular cross-sections using closed moulds. But the foam did not harden due to limited air access and humidity. An alternative is to use two-component mounting foam which can be used in a closed space, but this does not solve the problem of removing the specimen from the mould due to adhesion of the foam. Cutting the specimens out of the mould only solves this problem. The moulds can be easily cleaned for further use after specimen preparation. The method of removal from the mould (cutting out) also affects the shape of the specimen. Square specimens (cubes, bars, etc.) were much easier to remove from the moulds.

Removal of the specimen from the mould is complicated by the ability of the foam to stick to any readily available material. According to the manufacturer, the mounting foam used should not stick to teflon or silicone. There are several commercially available release agents on the market, but they are not used in this article. One option would be to use these materials to make the mould or to treat the surfaces that are in direct contact with the foam. The problem of hardening the foam in closed moulds was mentioned in the previous section. We assumed that a similar problem would occur when using, for example, silicone moulds. This option was not tested, but for some parts of the mould it could be a suitable alternative to 3D printing. On the other hand, the foam should adhere as well as possible to the clamping parts (tensile test specimen).

Tab. 2 shows the tensile modulus values for various materials found in the cited literature. To compare individual materials, it would be useful to use similar tests for other materials.

References	Material	Young's modulus [MPa]
[Kabir 2006]	PUR240	1600
[Jiang 2020]	RGD515/ 531	1200
[Zenkert 2009]	Rohacell WF51	75
[Morton 2020]	EPP foam	11
[Yousaf 2022]	PU unfiled	8.11
This contribution	PUMFD	1.9

Table 2. Comparison of the modulus of elasticity

In this paper, different specimens shapes are used than in the cited literature due to the production technology. The materials are also different and direct comparison is therefore complicated. Our intention for the future is to use experiments to identify material models of foams where whole specimens will be simulated using FEM. The input for the identification is values of force and displacement. This approach allows the use of more complex specimen shapes, but complicates comparison with the literature, where results are most often presented as a function of stress versus strain. Fig. 21 shows a comparison with expanded polystyrene (EPS) with density 6 and 15 kg/m^3 compressed at speed 3 mm/min (data taken from [Li 2021]). Our polyurethane foam (PUMFD), had a density of 28 kg/m^3 and was compressed at speed 4 mm/min.

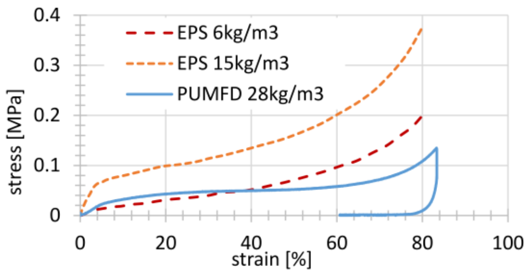

Figure 21. Comparison of compression tests

For the tensile test, the comparison is made with the material marked PU5 (see Fig. 22), where the data were taken from literature [Zmora-Murillo 2017].

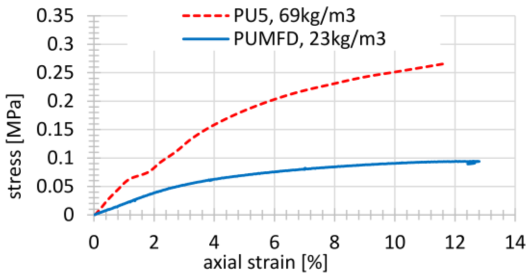

Figure 22. Comparison for tension test

For all tests, the measurements were performed with a testing machine and optically with the DIC method. From the results presented, it is expected that the measured data can be used to identify material parameters or to validate them.

Two different velocities were used in the compression experiments. However, for the future, we are considering the use of a Hopkinson testing machine capable of developing higher strain rates or the use of a temperature chamber to determine the effects of temperature on the mechanical behaviour of the foam.

The next planned approach, building on the present paper, can be summarised in the following points:

- Test more foam materials.
- Check the behaviour at higher strain rates.
- Test the behaviour at different temperatures.
- Test selected material models for foams, including the determination of material parameters.

The acquired knowledge will be then applied to:

- Selected manipulator arms designed by topological optimisation and frame structures made from prefabricated metal parts [Rojicek 2021/2] and filled by mounting foam.
- The effect of foams on selected properties (buckling, vibration, deflection, etc.) can be tested.

7 CONSLUSIONS

The results presented in this paper show that the proposed method is suitable for producing test specimens made from PU mounting foams The method can also be used for more complex shapes (e.g., tensile specimens in our case) or for foams of different composition. The experimental data can be used to determine their basic material properties. Mechanical properties of mounting foams are generally not available. Foams are characterised by a relatively large scatter of measured values, but for larger test series statistical processing methods can be used to find corresponding representative curves. In addition, the data obtained from DIC can be used to validate the results if required.

ACKNOWLEDGMENTS

This article was elaborated under support of the Research Center of Advanced Mechatronic Systems, reg. no. CZ.02.1.01/0.0/0.0/16_019/0000867, within the framework of the Operational Program for Research, Development, and Education.

REFERENCES

[Alpha SW 2022] X-Sight: Alpha SW [online]. Brno: X-Sight, 2022 [cit. 2022-05-25]. Available at: https://www.xsight.eu/alpha/

[Anirudh 2022] Anirudh, S., et al. Epoxy/glass syntactic foams for structural and functional application-A review. European Polymer Journal, 111163. ISSN:0014-3057. 2022

[Bhaduri 1994] Bhaduri, S. B. Science and technology of ceramic foams. Advanced Performance Materials, 1(3), 205-220. ISSN : 1572-8765. 1994

[Bhagavathula 2022] Bhagavathula, et al. Density, strain rate and strain effects on mechanical property evolution in polymeric foams. International Journal of Impact Engineering, 161, 104100. 2022

[Den Braven 2022] Den Braven: Montazni pena [online]. Uvalno: Den Braven Czech and Slovak, 2022 [cit. 2022-05-24]. Available at: https://denbraven.cz/produkt/montazni-pena/#

[Donnard 2018] Donnard, A., et al. Multiaxial experiments with radial loading paths on a polymeric foam. Polymer Testing, 67, 441-449. 2018

[Dukhan 2013] Dukhan, N. Metal foams: fundamentals and applications. DEStech Publications, Inc. ISBN: 9781605950143. 2013

[Eaves 2004] Eaves, D. Handbook of polymer foams. iSmithers Rapra Publishing. ISBN : 1859573886. 2004

[Gama 2004] Gama, N. V., et al. Polyurethane foams: Past, present, and future. Materials, Vol.11, No.10, pp1841. EISSN 1996-1944. 2004

[Gilchrist 2001] Gilchrist, A. and Mills, N. J. Impact deformation of rigid polymeric foams: experiments and FEA modelling. International journal of impact engineering, 25(8), 767-786. 2001

[Henriques 2020] Henriques, I. R., et al. Viscoelastic behavior of polymeric foams: Experiments and modeling. Mechanics of Materials, 148, 103506. 2020

[Huo 2016] Huo, W. L., et al. Highly porous zirconia ceramic foams with low thermal conductivity from particle-stabilized foams. Journal of the American Ceramic Society, 99(11), 3512-3515. ISSN:1551-2916. 2016

[Jiang 2020] Jiang, H., et al. Mechanical properties of 3D printed architected polymer foams under large deformation. Materials & Design, Vol.194. ISSN 0264-1275. 2020

[Kabir 2006] Kabir, M. E., et al. Tensile and fracture behavior of polymer foams. Materials Science and Engineering: A, 429(1-2), 225-235. 2006

[Kumar 1993] Kumar, V., et al. Microcellular polymers: novel materials for the 21st century. Cellular Polymers, Vol.12, No.3, pp 207-223. 1993

[Lee 2020] Lee, J. H., et al. Constitutive-damage modeling and computational implementation for simulation of elasto-viscoplastic-damage behavior of polymeric foams over a wide range of strain rates and temperatures. International Journal of Plasticity, 130, 102712. 2020

[Li 2021] Li, S. and Li, Q. M. Response of functionally graded polymeric foam under axial compression. International Journal of Mechanical Sciences, 210, 106750. 2021

[Marx 2017] Marx, J., et al. Overview of composite metal foams and their properties and performance. Advanced Engineering Materials, 19(11), 1600776. ISSN: 1527-2648. 2017

[Morton 2020] Morton, D.T., Reyes, A., Clausen A.H. and Hopperstas O. S. Mechanical response of low density expanded polypropylene foams in compression and tension at different loading rates and temperatures. Materials Today Communications. 2020, 23. ISSN 23524928. Available at: doi:10.1016/j.mtcomm.2020.100917. 2020

[Paska 2020] Paska, Z., et al. Methodology of arm design for mobile robot manipulator using topological optimization. MM Science Journal. 3918-3925. ISSN 18031269. Available at: doi:10.17973/MMSJ.2020_06_2020008. 2020.

[Paska 2021] Paska, Z., et al. Load capacity of helicol ® inserts in abs M30 material used for additive manufacturing. MM Science Journal., 5414-5420. ISSN 18031269.

Available at: doi:10.17973/MMSJ.2021_12_2021111. 2021

[Prusa 2022] PRUSA RESEARCH by JOSEF PRUSA: Prusament PETG [online]. Prague: Prusa Research, 2022 [cit. 2022-05-24]. Available at: https://www.prusa3d.com/category/prusament-petg/?page=2

[Rojicek 2021] Rojicek, J., et al. Optimization of a Truss Structure Used to Design of the Manipulator Arm from a Set of Components. Applied Sciences. 2021, 11(21). ISSN 2076-3417. Available at: doi:10.3390/app112110193. 2021

[Rojicek 2021/2] Rojicek, J., et al. Material model identification from set of experiments and validation by DIC. Mathematics and Computers in Simulation. 2021, 189, 339-367. ISSN 03784754. Available at: doi:10.1016/j.matcom.2021.04.007. 2021

[Rojicek 2021/3] Rojicek, J., et al. Material model identification from set of experiments and validation by DIC. Mathematics and Computers in Simulation. 2021, 189, 339-367. ISSN 03784754. Available at: doi:10.1016/j.matcom.2021.04.007. 2021

[Singh 2018] Singh, S., et al. A survey of fabrication and application of metallic foams (1925–2017). Journal of Porous Materials, 25(2), 537-554. ISSN: 1573-4854. 2018

[SOUDAL 2011] SOUDAL: SOUDAFOAM COMFORT [online]. Frydek-Mistek: Soudal Czech Republic, ©2011 [cit. 2022-05-31]. Available at: https://www.soudal.cz/produkt/soudafoam-comfort

[Srivastava 2014] Srivastava, V. and Srivastava, R. On the polymeric foams: modeling and properties. Journal of Materials Science. 2014, 49(7), 2681-2692. ISSN 0022-2461. Available at: doi:10.1007/s10853-013-7974-5. 2014

[Testometric 2021] Testometric Co. Ltd. Testometric materials testing machines. 50KN MACHINES, 2021, [online]. [cit. 23.7.2021]. Available from <http://www.testometric.co.uk/50kn/>

[Wu 2010] Wu, Z., et al. Experimental and numerical studies of the pressure drop in ceramic foams for volumetric solar receiver applications. Applied Energy, 87(2), 504-513. ISSN 0306-2619. 2010

[Yang 2015] Yang, X. H., et al. A simplistic unit cell model for sound absorption of cellular foams with fully/semi-open cells. Composites Science and Technology, 118, 276-283. ISSN:0266-3538. 2015

[Yousaf 2022] Yousaf, Z., et al. Tensile properties of all-polymeric syntactic foam composites: experimental characterization and mathematical modelling. Composites Part B: Engineering, 231, 109556. 2022

[Zenkert 2009] Zenkert, D. and Burman, M. Tension, compression and shear fatigue of a closed cell polymer foam. Composites Science and Technology. 2009, 69(6), 785-792. ISSN 02663538. Available at: doi:10.1016/j.compscitech.2008.04.017. 2009

[Zmora-Murillo 2017] Zmora-Murillo, L. D., et al. Thermal-Mechanical Characterization of Polyurethane Rigid Foams: Effect of Modifying Bio-Polyol Content in Isocyanate Prepolymers. Journal of Renewable Materials. 2017, **5**(3), 220-230. ISSN 2164-6325. Available at: doi:10.7569/JRM.2017.634112

CONTACTS:

Ing. Zbynek Paska
Department of Applied Mechanics
VSB – Technical University of Ostrava
Faculty of Mechanical Engineering
17. listopadu 2172/15
708 33 Ostrava – Poruba, Czech Republic
e-mail zbynek.paska@vsb.cz